DEVELOPMENT AND UNDERSTANDING OF THE INTRINSIC AND DOPED AMORPHOUS EMITTER-LAYER STACKS FOR SILICON HETEROJUNCTION SOLAR CELLS

D. Pysch, C. Meinhardt, M. Hermle, S. W. Glunz
Fraunhofer Institute for Solar Energy Systems, Heidenhofstr. 2, D-79110 Freiburg, Germany
Phone: +49-761-4588-5287; Fax: +49-761-4588-9250; email: damian.pysch@ise.fraunhofer.de

ABSTRACT: Comparison of the open-circuit voltage V_{oc} determined by *suns*V_{oc} to the implied voltage $V_{oc,impl}$ determined by transient QSSPC lifetime measurements can lead to a quick and easy analysis and characterization of silicon heterojunction (SHJ) solar cells, especially in regard to finding the optimum doping concentration of the emitter layer (stack system). The $V_{oc,impl}$ represents the interface passivation quality. The *suns*V_{oc} value gives us additionally a measure of the apparent band-bending. Increasing the concentration of doping gases during the deposition of e.g. a-Si:H(p) reduces the interface passivation quality ($V_{oc,impl}$) and increases the band-bending (*suns*V_{oc} value). The best trade off is realized when the ratio of *suns*V_{oc} to $V_{oc,impl}$ (V_{oc} trade off ζ) first comes to a saturation value near 1, while increasing the doping concentration. For a-Si:H(p) layers the pseudo fill factor *PFF* is found to be dependent on the doping concentration, too. Thus, the maximum value obtained for the *PFF* *suns*V_{oc} product is taken as a measure for the optimal doping concentration of a-Si:H(p) emitter layers. This approaches are applied to answer the following questions: i) what is the optimum doping concentration for an a-Si:H(n) emitter layer vs. an a-Si:H(i & n) emitter layer stack? ii) what is the best doping concentration of the a-Si:H(p) layer in an a-Si:H(i & p) emitter layer stack system including a variation of the a-Si:H(i) as well as the a-Si:H(p) layer thickness?
Keywords: silicon, heterojunction, amorphous silicon.

1 INTRODUCTION

Silicon heterojunction (SHJ) solar cells are known to have the potential to produce open-circuit voltages above 700 mV [1-3]. In order to obtain such high voltages we need to guarantee a good passivation of the interface between the amorphous and the crystalline silicon (c-Si(n or p)), as well as an optimal doping of the emitter layer a-Si:H(p or n) [4]. Currently the best performing SHJ solar cell approach is the HIT concept [1], where a hydrogenated, intrinsic amorphous a-Si:H(i) layer passivates the interface, while the doped amorphous layer (a-Si:H(p or n)) forms the actual emitter/BSF (back surface field) and is responsible for a sufficient band banding (see Fig.1). The band banding in a SHJ solar cell can roughly be understood as a built in voltage in diffused emitter silicon solar cells.

The challenge in the development of SHJ solar cells is that both, the interface passivation and the optimal band bending need to be optimized at the same time. It is known from advanced characterization as near-UV photoemission spectroscopy and surface photo voltage measurements that an excessively high doping of the a-Si:H(n) layer can lead to a reduction of the open-circuit voltage, due to an increasing defect concentration in the a-Si:H(n) layer [4-6]. An easy approach to monitor the influence of a variation of the doping concentration of the emitter layer or a variation of the thickness of the a-Si:H(i) layer influencing the band bending and passivation quality, is to compare the calculated, lifetime-based implied voltage with the actually measured *suns*V_{oc} voltage, affected by lifetime and band bending.

Combining these measurements, which can be performed quickly, with simple setups, makes the physical analysis and optimization of SHJ solar cells fast and effective.

2 EXPERIMENTAL

Lifetime (in transient mode) and *suns*V_{oc} measurements were performed with a *suns*V_{oc} and QSSPC measurement setup by Sinton Consulting [7, 8].

The thickness of the a-Si:H layers were determined by spectroscopic ellipsometry. All measurements shown were performed using a J.A. Woolam C. VASE rotating analyzer ellipsometer. The angle of incidence was 70° and a Tauc-Lorentz-model was used to fit the data [9]. The error of the thickness measurement was determined by comparison of spectral ellipsometry and transmission electron microscopy measurements to around 0.5 nm [9].

All a-Si:H(i,n,p), and ITO layers were deposited using a "System 100 Pro", a multi PECVD chamber cluster tool by Oxford Instruments.

For this investigation we processed full heterojunction V_{oc}-samples (see Fig. 1) on flat and textured, n- and p-type crystalline silicon c-Si wafers (FZ, 1Ω cm, 210 µm). All wafers were wet-chemically oxidised in HNO_3, which has been removed by a short 1%-HF dip prior to the a-Si:H(i) deposition [10, 11]. The rear side of all V_{oc}-samples (c-Si(n & p)) is made of 5nm a-Si:H(i), a 15 nm of n- or p-doped amorphous silicon, and 80 nm of ITO. On the front side the thickness of the a-Si:H(i) layer has been varied. For the emitter a-Si:H(p or n) layer, we varied the thickness as well as the doping gas concentration of diborane B_2H_6 or phosphine PH_3. The doping gases were diluted in H_2 with a concentration of 1% B_2H_6 in H_2 and 0.27% PH_3, also in H_2.

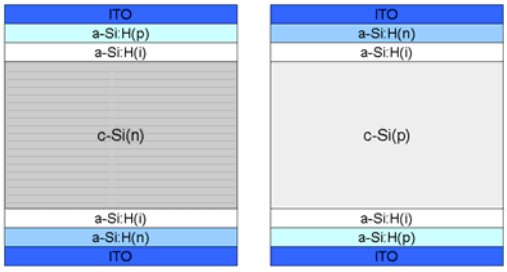

Fig.1 Structure of a V_{oc}-samples on an n- and p-type c-Si wafer. Such V_{oc}-samples were used for all investigations in this publication.

3 RESULTS

3.1 Optimum doping concentration of B_2H_6 in an a-Si:H(p) layer in an a-Si:H(i + p) emitter stack

For the optimization of the B_2H_6 concentration during the deposition of a-Si:H(p), we substituted the H_2 gas flow, which was already present for the optimized a-Si:H(i) deposition process [12] subsequently with the doping gas B_2H_6 diluted in H_2. Thus, the total gas flow and ration of H_2 to SiH_4 remained constant, with only the concentration of B_2H_6 is being varied.

One could process fully metalized SHJ solar cells, and measure the resulting V_{oc}. With the saturation of the V_{oc} value with increasing doping concentration one would get the optimum doping gas flow, too. For SHJ solar cells including an ITO layer on the front and back side, it is however, not necessary to process the metallization of the solar cells. It is possible to measure the V_{oc} value and the shape of the resulting series resistance free IV-curve represented by the pseudo fill factor *PFF* using a Sinton Consulting *suns*V_{oc} setup. If we further conduct a lifetime measurement using the Sinton Consulting QSSPC (in transient mode), we can determine the minority carrier density at an illumination density of one sun. This enables us to calculate the so-called implied voltage

$$V_{OC,impl} = \frac{k_B T}{q} \ln\left(\frac{p \cdot n - n_i^2}{n_i^2}\right). \qquad (1)$$

T represents the temperature, k_B the Boltzmann constant, q the elementary charge, p the minority carrier density, n the doping concentration of the n-wafer, and n_i the intrinsic carrier density of silicon (n_i=10^{10}cm^{-3}). Applying equation (1) to a p-type wafer SHJ solar cell, n is representing the minority carrier concentration, and p the wafer doping concentration. The implied voltage $V_{oc,impl}$ gives us a measure for the interface passivation and the splitting of the quasi Fermi level within the wafer. The *suns*V_{oc} value is a measure of interface passivation, too. However, we can additionally measure the apparent band bending realized by the doping gas. Thus, the *suns*V_{oc} value represents the quasi Fermi level splitting directly at the ITO contacts.

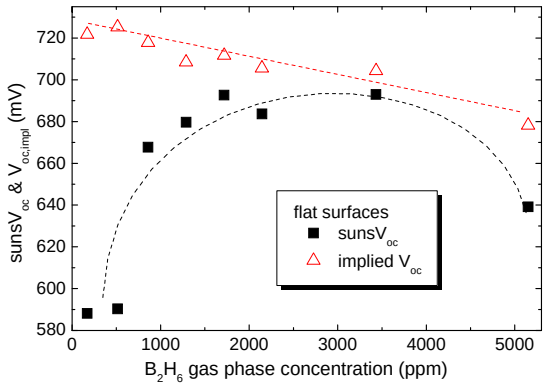

Figure 2: Dependence of the *suns*V_{oc} and $V_{oc,impl}$ measurements on the gas phase doping concentration of the a-Si:H(p) layer in an a-Si:H(i+p) layer stack. Lines are guides to the eye.

The rear sides of the V_{oc}-samples shown in Figure 2 consist of a layer stack as described in the experimental section. At the front side we deposited a 5 nm a-Si:H(i) layer, followed by 10 nm of a-Si:H(p) with different B_2H_6-H_2 concentrations, and an 80 nm ITO layer on top. The dependence of the *suns*V_{oc} and the $V_{oc,impl}$ value on an increasing B_2H_6 gas phase concentration (see Fig.2) shows an approximately linear decrease of the $V_{oc,impl}$ and thus of the interface passivation. The optimum doping gas phase concentration (highest *suns*V_{oc}) is found to be between 2000 and 3500 ppm of B_2H_6 in the total gas phase. We are now able to conclude that the best trade off between interface passivation decrease and increase of the band bending is in the region around 2000 and 3500 ppm of B_2H_6 in the deposition gas phase.

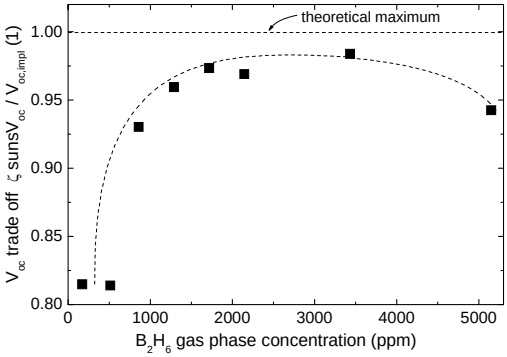

Figure 3: V_{oc} trade off ζ (*suns*V_{oc} / $V_{oc,impl}$) in dependence of the doping gas phase concentration of the a-Si:H(p) layer. The best trade off ζ between the increase of the band-bending and the decrease of the interface passivation is in the region around 2000 and 3500 ppm where the trade off ζ reaches a saturation level. Since the *suns*V_{oc} can not be higher than the $V_{oc,impl}$, the ratio of 1 is the theoretical limit. The line is a guide to the eye.

Figure 3 shows the ratio of *suns*V_{oc} and $V_{oc,impl}$ in dependence of the doping concentration of the a-Si:H(p) layer. This ratio will be cited as V_{oc} trade off ζ in the following. The ζ plot in Figure 3 shows the approach of the increasing band bending to the optimum value near 1 with increasing B_2H_6 gas phase concentration, where the Fermi level splitting at the ITO contacts and inside the wafer are approximatly the same. The best trade off between the increase of the band-bending and the decrease of the interface passivation is found in the region around 2000 and 3500 ppm, where ζ reaches a saturation level. Since the *suns*V_{oc} can not be higher than the $V_{oc,impl}$, the ratio of 1 is the theoretical limit.

In Figure 4 the influence of an increasing doping concentration of the a-Si:H(p) layer on the pseudo fill factor *PFF* is shown. We observe a continuous decrease of the *PFF* with increasing B_2H_6 concentration. This observation may be explained by an increasing defect density in the a-Si:H(p) layer caused by the increasing doping concentration. This interpretation is supported by the decreasing normalized lifetime for minority carrier concentrations below 10^{15} cm^{-3} (insert in Fig. 4).

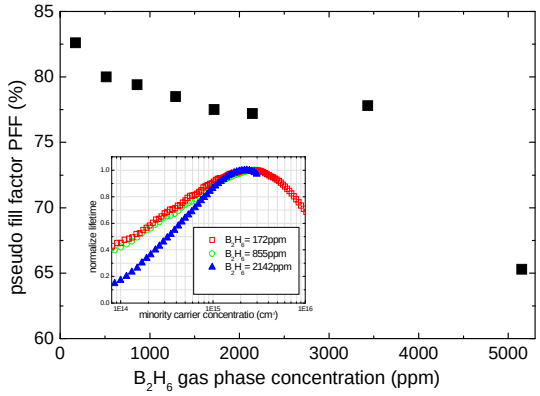

Figure 4: Dependence of the *PFF* on the gas phase doping concentration of a-Si:H(p). Inserted is the influence of the gas phase doping concentration on the dependence of the normalized lifetime on the minority carrier concentration.

Knowing the doping dependence of the *PPF* (Fig. 4) and $sunsV_{oc}$ (Fig. 2), we can multiply both values and end up with good measure for the optimum doping concentration, which is again between 2000 and 3500 ppm (see Fig. 5).

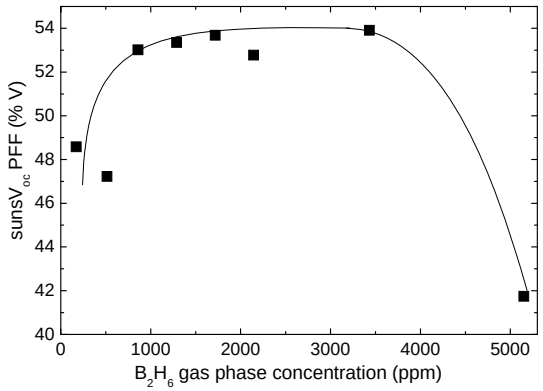

Figure 5: Dependence of the pseudo fill factor *PFF* times $sunsV_{oc}$ product on the doping concentration of the a-Si:H(p) layer. The line is a guide to the eye.

3.2 Optimization of the a-Si:H(i & p) layer thickness and the doping concentration of B_2H_6 for a-Si:H(p)

In section 3.1, we presented our results of an optimization of a 5nm a-Si:H(i) and 10 nm a-Si:H(p) emitter stack in regard to the optimal gas phase doping concentration. In this section we investigate the influence on the $sunsV_{oc}$ and $V_{oc,impl}$ caused by a reduction of the a-Si:H(i) layer thickness and a variation of the a-Si:H(p) layer thickness from 5 to 20 nm.

In Figure 6 the results for the a-Si:H(i & p) layer thickness variation are shown for two different gas phase doping concentrations: the optimum concentration of 2100 ppm (see sec. 3.1), and a lower bound of 1600 ppm. It seems not to matter which doping concentration is applied for a-Si:H(p) layers down to 12 nm, for both a-Si:H(i) thicknesses (arrow (a) in Fig. 6). For an a-Si:H(i) layer thickness of 6 nm the $sunsV_{oc}$ values start to saturate for a-Si:H(p) layer thicknesses above 8 nm (arrow (b) in Fig. 6). Once the a-Si:H(p) layer is reduced to 5 nm, the higher doping concentration improves the performance significantly.

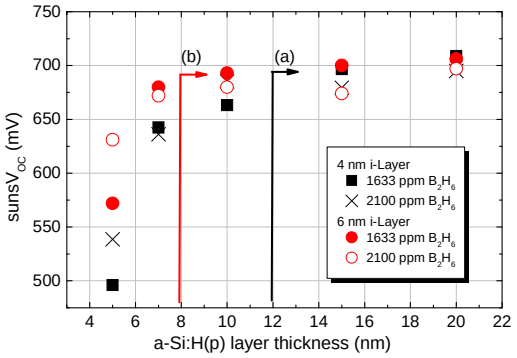

Figure 6: Dependence of $sunsV_{oc}$ on the thickness of the a-Si:H(i), a-Si:H(p) and the doping concentration. The arrows (a) and (b) indicate saturation levels of the 4 and 6 nm thick a-Si:H(i) layer, respectively.

Figure 7 shows the V_{oc} trade off ζ and makes the trends mentioned above even more obvious. There is a reduction of ζ for a-Si:H(p) layers below 12 nm observable, for 4nm a-Si:H(i) layer thickness and the both doping concentration. For the 6 nm a-Si:H(i) layer thickness, ζ starts to decline below 1 for an a-Si:H(p) layer thickness lower than 8 nm. Plotting the V_{oc} trade off ζ revealed that with a reduction of the a-Si:H(i), a-Si:H(p) layer thickness, and doping concentration at the same time, we end up with a decrease of the internal band-bending. Thus, for an a-Si:H(i & p) stack emitter, it seems to be evident to increase the doping concentration for very thin stack thicknesses.

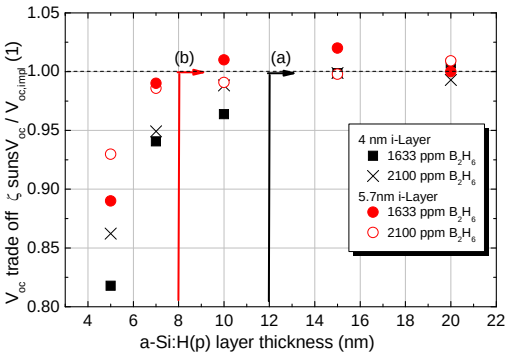

Figure 7: Dependence of the ratio between the $sunsV_{oc}$ and the $V_{oc,impl}$ on the thickness of the a-Si:H(i), a-Si:H(p) and the doping concentration. The arrows (a) and (b) indicate saturation levels of the 4 and 6 nm thick a-Si:H(i) layer, respectively.

3.3 Optimum doping concentration of PH_3 for a-Si:H(n)

Next we applied the same procedure for the optimization of the a-Si:H(n) emitter layer in regard to the gas phase PH_3 concentration. In Figure 8 a stack of a 5 nm a-Si:H(i) and 10nm a-Si:H(n) layers (bottom) is compared to a 15 nm pure a-Si(n) emitter layer (top). This experiment was conducted on 1 Ω cm FZ p-type material.

Figure 8 shows that the increase of the PH_3 gas phase concentration is equally harmful on the interface passivation for V_{oc}-samples with and without an a-Si:H(i)

layer. The optimum doping concentration for the a-Si:H(i+n) emitter stack is around 1000 ppm of PH_3 in the deposition gas phase ($V_{oc,best}$=716mV, bottom of Fig. 8, bottom). For the pure a-Si:H(n) emitter, the optimum doping concentration is around 500 ppm of PH_3 in the deposition gas phase ($V_{oc,best}$=703mV, top of Fig 8 top). This results do not agree well with the investigation published by Korte et al. [5]. The authors observed concentration of around 2000 ppm of PH_3 in the total gas phase to be best for a pure a-Si:H(n) emitter. The difference may be explained by the use off different deposition techniques or processes regimes. Korte et al. used a standard parallel plate set up. We deposited the a-Si:H(n) layer using an inductively coupled plasma, which is know for the creation very dense plasma [13]. In order to be able to make a final decision in regard to which emitter is best; the pure a-Si:H(n) or the a-Si:H(i+n) stack, metalized solar cell has to be processed, since the a-Si:H(i+n) stack should result in a lower *FF* due to the low conductivity of the a-Si:H(i) layer [14]. For PH_3 doped a-Si:H(n) layers we observed no clear dependence of the PFF on the doping concentration.

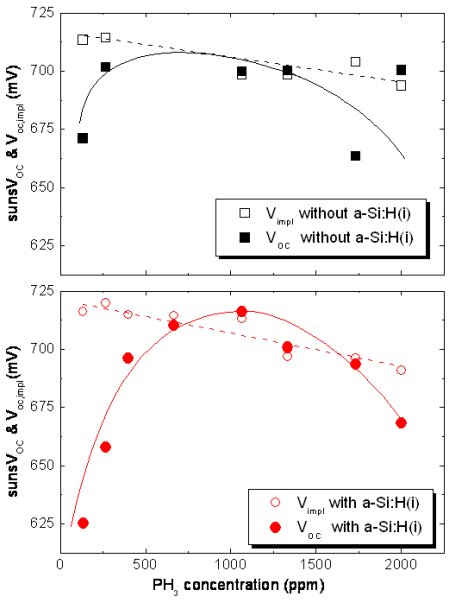

Figure 8: Dependence of the $sunsV_{oc}$ and $V_{oc,impl}$ on the doping concentration of the a-Si:H(n) layer and a-Si:H(i+n) stack. Lines are guides to the eye.

3 CONCLUSION

We presented in this publication that a comparison of V_{oc} values determined by $sunsV_{oc}$ to implied voltage $V_{oc,impl}$ (determined by transient QSSPC lifetime), can lead to a quick and easy analysis and characterization of silicon heterojunction (SHJ) solar cells, especially in regard to finding the optimum doping gas phase concentration of the emitter layer (stack system). The $V_{oc,impl}$ represents the interface passivation quality. The $sunsV_{oc}$ value gives us an additional measure of the apparent band bending. Increasing the concentration of dopants during the deposition of e.g. for a-Si:H(p) reduces the interface passivation quality ($V_{oc,impl}$) and increases the band bending ($sunsV_{oc}$ value). The best V_{oc} trade off ζ is realized when the ratio of $sunsV_{oc}$ to $V_{oc,impl}$ first comes to an saturation point near one with an increasing doping concentration or the product of *PFF* times $sunsV_{OC}$ reaches a maximum value (for emitters containing an a-Si:H(p)). Too high doping concentrations impair both $sunsV_{oc}$ and $V_{oc,impl}$. By applying this characterization approach, we have been able to show that an a-Si:H(i & n) emitter stack performs slightly better compared to a pure a-Si:H(n) emitter (including a lower optimum doping concentration). However, the question remains, whether a higher conductivity of pure a-Si:H(n) emitters can lead to a higher *FF* and thus to higher efficiency. Next we could show that, for an a-Si:H(i & p) emitter, a reduction of the thickness of both layers has to be compensated by an increase of the doping concentration in the a-Si:H(p) layer.

4 ACKNOLEGMENT

The authors would like to thank S. Seitz, T. Leimenstoll, A. Stifel, T. Boritzka, I. Druschke, F. Schaetzle, A. Filipovic, and E. Schäffer for process technology, simulation support and measurements. The work has been supported by the German Federal Ministry for the Environment, Nature Conservation and Nuclear Safety under contract number 0329849A „Th-ETA“.

5 REFERENCES

[1] T. Sawada, et al., Proceedings of the 1st World Conference on Photovoltaic Energy Conversion Hawaii, USA (1994) 1219.
[2] S. Taira, et al., Proceedings of the 22nd European Photovoltaic Solar Energy Conference Milan, Italy (2007) 932.
[3] S. Olibet, et al., Proceedings of the 23rd European Photovoltaic Solar Energy Conference, Valencia, Spain (2008) 1140.
[4] L. Korte and M. Schmidt, Journal of Non-Crystalline Solids **354** 2138 (2008).
[5] L. Korte, et al., Solar Energy Materials & Solar Cells **93** 905 (2009).
[6] A. Laades. in Fakultät II -Mathematik und Naturwissenschaften, pp. 129, Technische Universität Berlin 2005.
[7] R.A. Sinton, et al., Proceedings of the 25th IEEE Photovoltaic Specialists Conference, Washington DC, USA (1996) 457.
[8] R.A. Sinton and A. Cuevas, Proceedings of the 16th European Photovoltaic Solar Energy Conference, Glasgow, UK (2000) 1152.
[9] A. Richter, et al., Proceedings of the 23rd European Photovoltaic Solar Energy Conference, Valencia, Spain (2008) 1724.
[10] J.-P. Becker, et al., Proceedings of the 24th European Photovoltaic Solar Energy Conference, Hamburg, Germany (2009) 1123.
[11] H. Angermann, et al., Central European Journal of Physics **7** 363 (2009).
[12] D. Pysch, et al., Proceedings of the 24th European Photovoltaic Solar Energy Conference, Hamburg, Germany (2009) 1580.

[13] S.J. Schreiber. in Department of Engineering, pp. 177, University of Cambridge, Cambridge 2001.

[14] C. Meinhardt, et al., presented at this conference.